



Article

The Effect of Recycled Citrogypsum as a Supplementary Mineral Additive on the Physical and Mechanical Performance of Granulated Blast Furnace Slag-Based Alkali-Activated Binders

Natalia I. Kozhukhova ^{1,2,*} , Nataliya I. Alfimova ^{3,4} , Marina I. Kozhukhova ⁵, Ivan S. Nikulin ^{6,7}, Roman A. Glazkov ¹ and Anna I. Kolomytceva ¹

- ¹ Department of Material Science and Material Technology, Belgorod State Technological University Named after V.G. Shukhov, 46 Kostyukova Str., 308012 Belgorod, Russia
 - ² Laboratory of Advanced Materials and Technologies, Belgorod National Research University, 85 Pobedy Str., 308015 Belgorod, Russia
 - ³ Department of Material Science, Products and Structures, Belgorod State Technological University Named after V.G. Shukhov, 46 Kostyukova Str., 308012 Belgorod, Russia
 - ⁴ Research and Education Center Additive Technologies, National Research Tomsk State University, 36 Lenin Ave., 634050 Tomsk, Russia
 - ⁵ Department of Civil & Environmental Engineering, University of Wisconsin Milwaukee, 3200 N Cramer Str., Milwaukee, WI 53201, USA
 - ⁶ Engineering Center NRU "BelSU", Belgorod, 2a/712, Koroleva Str., 308015 Belgorod, Russia
 - ⁷ Fund of Innovative Scientific Technologies, 1, Room 3.3 Perspektivnaya Str. (Novosadovy Mkr.), 308518 Belgorod, Russia
- * Correspondence: kozhuhovanata@yandex.ru; Tel.: +7-9511420654



Citation: Kozhukhova, N.I.; Alfimova, N.I.; Kozhukhova, M.I.; Nikulin, I.S.; Glazkov, R.A.; Kolomytceva, A.I. The Effect of Recycled Citrogypsum as a Supplementary Mineral Additive on the Physical and Mechanical Performance of Granulated Blast Furnace Slag-Based Alkali-Activated Binders. *Recycling* **2023**, *8*, 22. <https://doi.org/10.3390/recycling8010022>

Academic Editor: Dariusz Mierzwiński

Received: 23 December 2022

Revised: 3 February 2023

Accepted: 3 February 2023

Published: 7 February 2023



Copyright: © 2023 by the authors. Licensee MDPI, Basel, Switzerland. This article is an open access article distributed under the terms and conditions of the Creative Commons Attribution (CC BY) license (<https://creativecommons.org/licenses/by/4.0/>).

Abstract: In the last decades, gypsum-bearing industrial wastes become one of the common globally produced industrial and domestic wastes that are currently recycled and further utilized. In this study, the gypsum-bearing waste citrogypsum was used as a Ca^{2+} -containing component to modify the properties of alkali-activated cement (AAC) based on granulated blast-furnace slag (GBFS). Citrogypsum was used in different AAC mixes activated with three different alkaline components: Na_2CO_3 , NaOH , and Na_2SiO_3 . Laser granulometry was applied to assess the granulometric characteristics of citrogypsum and GBFS. Specific gravity (SG), compressive strength, and water resistance were tested to evaluate the effect of citrogypsum on the physical and strength performance of AAC. Experimental results obtained over 4-day to 28-day time periods for the studied AACs showed that the addition of citrogypsum had a detrimental effect on the properties of AAC mixes, where decreases in compressive strength between 1 and 100%, decreases in specific gravity between 4 and 30%, and decreases in water resistance between 12 and 100% were observed. It was determined that AAC mixes modified with citrogypsum cured in ambient conditions had compressive strength values 61% to 90% lower than those cured in hydrothermal conditions. In terms of strength performance, specific gravity and water resistance, citrogypsum showed the greatest effect on AAC mixes activated with NaOH , and to a lesser extent, on mixes activated with Na_2CO_3 . The highest water resistance value of 0.77 was observed for the AAC mixes activated with Na_2CO_3 cured in ambient conditions, and when cured in hydrothermal conditions, the highest water resistance reached up to 0.84 for the AAC mixes activated with NaOH . It was observed that the type of alkaline activator and curing conditions are both crucial factors that govern the response of citrogypsum as a supplementary mineral additive in GBFS-based AAC mixes in regard to compressive strength, specific gravity and water resistance.

Keywords: alkali-activated cement (AAC); granulated blast furnace slag (GBFS); citrogypsum supplementary mineral additive; compressive strength; specific gravity; water resistance

1. Introduction

With the development of civilization and the growth of the world's population, one of the biggest environmental problems is the constantly increasing consumption of natural mineral and energy resources. The construction industry is now one of the leading consumers as it requires a large number of natural resources for building and production of construction materials [1–3].

At the same time, there are large reserves of underutilized industrial and municipal waste products that require recycling. The annual production volume of these materials is constantly growing.

Since most of the pollutants such as heavy metals and toxic polymers are prone to leaching from solid wastes into soils and aquatic ecosystems, the harmful effects of these pollutants can adversely affect aquatic biota [4–8]. However, there are no standardized tests to assess the environmental viability of solid waste treatment processes.

To date, a number of studies investigating useful, efficient, and safe approaches for recycling of solid-phase waste in various industries, including construction have been carried out [9–14].

It is noted that, after clay materials, gypsum is the second largest source of construction and demolition waste that is successfully recycled [15,16].

In past research [17], comparative studies were performed with a focus on assessing the economic and environmental benefits of using natural gypsum and gypsum waste in building materials. The outcomes of this study demonstrate that recycled gypsum (RG) has environmental benefits in all assessed environmental impact categories when industrial gypsum waste (GW) was transported up to 50 km to the processing plant. The study shows that the processing of RG and GW consumes less than 65% of the energy required to produce natural gypsum (NG) and emits less than 65% of the greenhouse gases generated in the NG manufacturing process. In addition, a reduction in carcinogenic exposure of up to 35% has been observed during the production and use of RG and GW.

There are some industrial gypsum-bearing wastes such as by-products from citric acid production, phosphate fertilizers, the coal combustion flue gas desulfurization process, etc. that can be recycled and used as a substitute for natural gypsum [11,15–17]. Very little research has been conducted to analyze the environmental impact of using RG produced from recycled drywall. At the same time, it was found that 65–80% of energy reduction can be achieved by using RG instead of a natural analogue. Research works [18,19] have proposed the use of gypsum raw materials processed from the drywall as an alternative to natural gypsum in the production of Ordinary Portland Cement (OPC). The results showed that the properties of OPC using both types of gypsum raw materials were similar.

Another study [17] explored the potential of using ceramic blocks produced from various proportions of clay, OPC, and GW. The results show that adding 20% GW to ceramic blocks can provide an effective replacement for clay in ceramic industry.

The main impact of GW use relates to conserving natural resources since the recycling of RG requires the same technological operations as for natural gypsum manufacturing (i.e., crushing, grinding, firing) [20]. One such alternative source of natural gypsum can be phosphogypsum (PG), which is a by-product of phosphate fertilizer production in the form of calcium sulfate [11].

A new and promising binding system based on gypsum has been proposed, consisting of three components: gypsum, OPC, and pozzolan [21], in which PG is used as the main binding component (up to 75 wt.%) instead of OPC. According to the authors' report, the production of this binder using PG can reduce energy costs by up to 30%, as well as reduce CO₂ emissions by 57% while maintaining the same characteristics of the final material.

The work [22] describes technological options for the recycling of PG as a combined system blended with OPC and fly ash for soil stabilization or as blended cements.

One of the most common types of GW is Flue Gas Desulphurization (FGD) gypsum, which is a product of the flue gas desulphurization process at coal-fired power plants [23].

This product is characterized by improved insulating properties and fire resistance of panels vs. panels based on NG and shows improved thermal conductivity of gypsum plasters [24].

The opportunities for recycling and utilization of citrogypsum in several industries were highlighted in a number of research studies [25–28]. Voropaev V. et al. [25] investigated the possibility to use citrogypsum in agriculture as an effective fertilizer, soil amendment and in composting of animal manure.

Kostić-Pulek A et al. [26] proposed a method to synthesize α -hemihydrate of CaSO_4 from citrogypsum using a suspending process.

Ozkul M.H. [27] demonstrated that citrogypsum can be successfully utilized as a set retarder in portland cement systems without negative effects on strength characteristics.

In the study [28], the authors investigated the effect of citrogypsum on rheological properties when used in electrometallurgical slag-based alkali activated binders.

A number of studies show that gypsum-bearing industrial wastes are currently used in a wide range of applications in the construction industry, agriculture and other industries, which supports the efficiency of these materials from the view of recyclability and further utilization as raw components and precursors.

The production of alkali-activated cement (AAC) is among the emerging promising applications for gypsum-bearing waste products in the construction industry. Such a great interest in this class of cementitious systems is explained by the possibility of using a wide range of by-products and industrial waste as the main reactive aluminosilicate raw material.

Thus, fly ash from coal power plants with a high and low content of calcium oxide CaO (fly ash class C and F, respectively) is actively used in AAC. Type F fly ash is more accessible than type C. However, one of the main obstacles associated with the use of alkali-activated fly ash as a binder component is that a high temperature from at least 50 °C to 85 °C is required for curing [29,30].

Metallurgical slags are more popular and efficient raw materials for production of AAC because they contain a large amount of Ca^{2+} cations, which allows saving on alkaline activators due to their content in aluminosilicate raw materials. The most commonly used slag activator is sodium silicate Na_2SiO_3 , which provides fast hardening of the binder system, even at low temperatures [31].

In addition to industrial wastes, natural and synthetic aluminosilicates are used for AAC production. Therefore, when using metakaolin, the highest strength is observed when a complex of activators consisting of sodium silicate Na_2SiO_3 , and sodium hydroxide NaOH is used. Alkaline activation using only NaOH provides lower strength characteristics [32]. However, under heat treatment up to 80 °C, the combination “metakaolin- NaOH ” demonstrates more intensive structure formation vs. the combination “metakaolin- Na_2SiO_3 ”.

The results obtained in the studies [33–35] showed that the use of Na_2CO_3 as a basic alkaline activator or as a component in the composition of a complex alkaline activators has a positive effect on the development of mechanical characteristics of AAC.

Collins F. et al. [34] presented results indicating that when slag is activated by a complex of alkaline components consisting of NaOH and Na_2CO_3 , the synthesized AAC develops early compressive strength comparable to that of OPC. A higher NaOH content in the “ NaOH - Na_2CO_3 ” complex, also leads to an intensification of the chemical reaction and, as a result, a more complete activation of slag in the early stages of hardening. However, this effect is practically absent at a later curing age.

According to the literature, the properties of AAC systems are fundamentally dependent on four main parameters: type of aluminosilicate component, type of activator (usually alkaline), curing conditions, and presence and type of modifying agent or modifier.

For example, GBFS-based AACs are classified a binders with mixed type of hardening, hydration and polymerization-polycondensation due to the chemical and mineral composition of raw materials. As for a hydraulic binder, such as portland cement, the most preferred hardening conditions are a high humidity of $\approx 95\%$ and a room temperature of 22 ± 3 °C, i.e., moist curing. On the other hand, for a binding system with a polymerization-

polycondensation type of hardening, such as geopolymer, the preferred curing conditions would be elevated temperature and low humidity, i.e., heat drying conditions. In addition, the type of alkaline activator also plays a significant role in the effectiveness of hardening.

Thus, GBFS-based AACs involve structure formation mechanisms requiring completely opposite curing conditions, that is, moist curing and heat drying conditions.

There are a number of research studies focused on the utilization of gypsum-bearing industrial waste in AAC mixes.

The work by Guo X. et al. [36] studied AAC multicomponent systems containing fly ash products and other Ca-containing additives such as portland cement and FGD gypsum. In this study, FGD gypsum was used as a Ca-containing additive, while NaOH and Na₂SiO₃ were used as alkaline activators. The resulting binder demonstrated a compressive strength of up to 80 MPa.

In the study by Maierdan Y. et al. [37], hemihydrate PG was used as part of the multicomponent mix together with portland cement, sodium metasilicate, ground granulated blast-furnace slag and waste river sludge for bricks production. In this case PG was used to dehydrate the waste river sludge.

Liu Z. et al. [38] in their study used gypsum-bearing sludge from a dyestuff-making plant in the manufacturing of unfired bricks based on slag cement.

Rashad A.M. in the work [39] explored the possibility of recycling calcined PG as a partial replacement of fly ash in AAC up to 15%. The authors observed that incorporation of PG in the fly ash-based AAC binder in the range of 5–10% can increase its thermal resistance.

The research work by Vaičiukynienė D. et al. [40] stated that the addition of PG in slag-based AAC binder shortened setting time when cured at room temperature.

The number of the reviewed research studies [36–40] reveals the level of research interest in finding opportunities for recycling and efficient utilization of gypsum bearing industrial waste products in AAC binders. However, the research is focused predominantly on utilization of PG, whereas the studies devoted to the use of other types of gypsum-bearing industrial waste materials in AAC binders are very limited.

The objective of this study is to observe the effect of hardening conditions and types of alkaline activators in GBFS-based AAC binders using recycled citrogypsum as a supplementary mineral additive and to evaluate its response to specific gravity, compressive strength as well as water resistance performance of the binders over time.

2. Results and Discussion

2.1. Compressive Strength and Specific Gravity of AAC

In this study, the values of SG and compressive strength were determined for all experimental mixes at the ages of 4, 7, and 28 days.

Citrogypsum was used in this study as a supplementary mineral additive with the aim to intensify formation structure and so accelerate strength development. To do so, the tendency of compressive strength development and change in values of SG for the experimental mixes of AAC over time were observed. The results are presented in Table 1 and Figure 1.

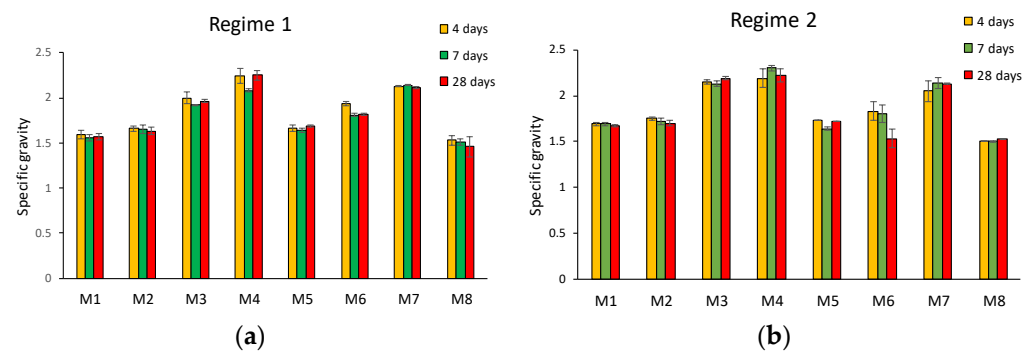
The rate of strength development, as depicted in Table 2, shows that the mixes M5, M6, and M8 cured in both Regimes 1 and 2, as well as M3 cured in Regime 1, and M4 and M7 cured in Regime 2 had gradual strength development throughout the 28 days study period.

However, the M4 and M7 specimens activated with NaOH, regardless of the curing regime, and the M3 specimen cured in Regime 2 gained at least 70% of the 28-day strength after 4 days of curing.

As depicted on Figure 1, the SG values for the mixes M4, M6, and M8 varied significantly as different curing regimes were applied. In the case of curing in Regime 1, a drastic drop in density was observed in the time interval from 4 to 7 days, followed by a gradual densification of the mixes M4 and M6, whereas mix M8 demonstrated a further reduction in specific gravity.

Table 1. Compressive strength of AAC mixes cured in different regimes.

Sample ID	Compressive Strength, MPa					
	Regime 1			Regime 2		
	4 d	7 d	28 d	4 d	7 d	28 d
M1	0	0	0	0	0	0
M2	0	0	0	0	0	0.257
M3	1.19	1.87	4.64	34.2	47.3	48.4
M4	23.4	28	32.19	29.9	29.2	37.5
M5	0.45	0.87	1.83	0.5	0.62	2.56
M6	0.55	0.39	0.55	0.1	0	0.1
M7	22	26.2	29.2	27.5	30	37
M8	0.13	0.44	0.83	0.1	0.25	0.81

**Figure 1.** Specific gravity of the AAC over time after curing under: (a) Regime 1 and (b) Regime 2.**Table 2.** Mix design of the AAC compositions.

Mix Design, % wt.						W/S Ratio *
Sample ID	GBFS	Citrogypsum	Alkaline Activator			
			Na ₂ CO ₃	NaOH	Na ₂ SiO ₃	
M1	100	—	—	—	—	0.21
M2	95	5	—	—	—	0.21
M3	95	—	5	—	—	0.2
M4	95	—	—	5	—	0.2
M5	95	—	—	—	5	0.21
M6	90	5	5	—	—	0.2
M7	90	5	—	5	—	0.2
M8	90	5	—	—	5	0.27

* The W/S ratio was calculated as the ratio of amount of water to the amount of the remaining solid components, including alkaline activator.

When curing Regime 2 was applied, the reverse effect was observed for the same mixes. In this case, in the time interval from 4 to 7 days of curing, mix M4 had a sharp increase in SG of 5%, followed by a gradual drop in the value until it almost reached the initial value by 28 days of curing. At the same time, M6, exhibited a slight drop in SG of less than 1% followed by an increase to 3% in the time interval from 4 to 7 days.

The incorporation of the citrogypsum component leads to reduction in SG for M8 under both curing regimes.

The compressive strength and SG results for experimental mixes at 28 days of curing (Table 2) show that curing conditions, type of activating agent, and addition of citrogypsum had a dramatic effect on compressive strength and, to a lesser extent, on specific gravity.

At the same time, the zero compressive strength values for the reference mixes M1 and M2 show that the absence of any alkaline activator in AAC leads to weak chemical

interaction between water and GBFS, even in the presence of citrogypsum, which contains the alkaline cations Ca^{2+} . This could be associated with the low reactivity of the GBFS used.

The results show that all the experimental AAC mixes cured in hydrothermal conditions revealed improved compressive strength vs. those cured in ambient conditions. The compressive strength was increased for the mixes M3, M4 and M7 by up to 10 times, whereas the strength for the mixes M5, M6, and M8 stayed practically unchanged, as shown in Table 2.

At the same time, the curing conditions had almost no effect on the SG for all experimental mixes (Figure 2), with the exception of mixes M3 and M6 activated with Na_2CO_3 . Specifically, for M3 without citrogypsum, the hydrothermal curing conditions contributed to the structure densification by 11%, which is consistent with an apparent increase in the compressive strength of this mix.

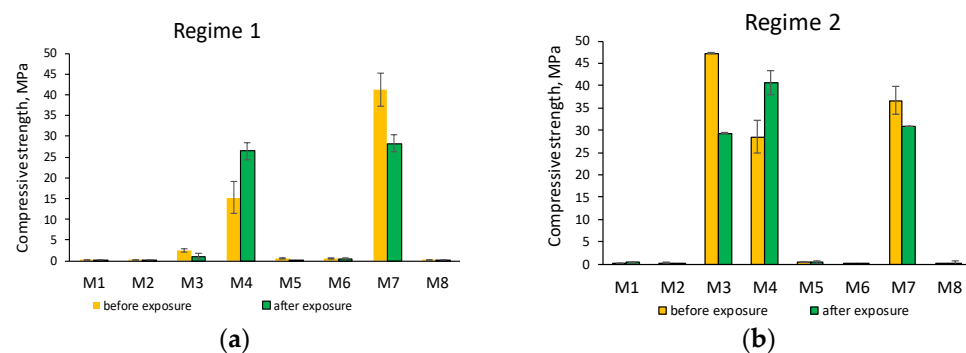


Figure 2. Compressive strength of AAC, before and after 24-h exposure in water cured in different regimes: (a) Regime 1; and (b) Regime 2.

M3 consists of GBFS activated with Na_2CO_3 . Na_2CO_3 is a source of the Na^+ cation. When dissolved in water, Na_2CO_3 creates alkaline media similar to that created by an NaOH alkaline activator. In fact, the alkaline media prompts mineral phases of GBFS, such as akermanite, helenite, anorthite and others, to react with Na^+ cations, resulting in formation of hydrates such as C-S-H, N-C-S-H and N-A-S-H. These hydrates form the structure of the cementitious matrix.

However, for M6 modified with citrogypsum, the opposite effect was observed, where curing in hydrothermal conditions, led to a loosening of the structure by about 8%.

The introduction of citrogypsum negatively affected the strength, initiating a drastic drop from 56% and almost to 0 for M6 and M8, regardless of curing conditions. For the M7 sample, the strength values remained unchanged when cured under either regime.

The influence of citrogypsum on AAC was manifested in a uniform decrease in SG for all experimental mixes, from 6 to 13% cured in Regime 1 and from 4% to 30% for the mixes cured in Regime 2.

The highest value of compressive strength was demonstrated by the mix M3 when cured in hydrothermal conditions (Regime 2). However, the mixes activated with Na_2CO_3 , such as M3 cured under Regime 1 and M6 cured under Regimes 1 and 2, showed significantly lower strength values from 0.1 to 5 MPa. Mixes M5 and M8 activated with Na_2SiO_3 showed extremely low strength values in the range of 2.5–0.8 MPa when subject to curing under both Regimes 1 and 2 and regardless of the presence/absence of the citrogypsum component.

Depending on the type of activating agent, the SG of experimental mixes was increased after curing under Regimes 1 and 2. The positive effect of the activating agents used in the AAC were ranked in the following sequence: $\text{Na}_2\text{SiO}_3 \rightarrow \text{Na}_2\text{CO}_3 \rightarrow \text{NaOH}$. At the same time, the difference between lowest and highest values of SG varied between 40 and 50%.

2.2. Water Resistance of AAC

It is known that gypsum binder has significant drawbacks for structural performance, among which is the low water resistance of the final product. In this regard, it seems important to study the effect of citrogypsum supplementation on the water resistance characteristics of AAC systems. To evaluate water resistance of the studied AAC, two sets of experimental mixes were prepared, each set included six cube samples of eight mixes. After molding, the first set of samples was placed in a hydrothermal curing chamber with an RH of $\approx 95\%$ and a temperature of $23 \pm 3^\circ\text{C}$ until the water resistance test was performed. After molding, the second set of samples was cured in ambient conditions at $\text{RH} \approx 42\%$ and temperature $23 \pm 3^\circ\text{C}$ for 4 h, then placed in a chamber to allow a heat treatment in the following regime: temperature rise in the chamber to 70°C for 1–1.5 h \rightarrow thermal conditioning at temperature of 70°C and humidity of $\approx 95\%$ for 24 h \rightarrow cooling in the chamber to ambient temperature for 1 h \rightarrow curing in ambient conditions with $\text{RH} \approx 42\%$ and temperature $23 \pm 3^\circ\text{C}$ until the water resistance test was performed. The experimental mixes were cured for 10 days before the test.

The water resistance test protocol involved the following steps:

- Three samples of each mix were placed in a container with water, where they were completely immersed in water to saturate for 24 h;
- Concurrently, the other set of the specimens were placed in an oven to dry at a temperature of $50 \pm 5^\circ\text{C}$ for 24 h.

After a 24-h exposure, the first set of the samples were removed from the water container and wiped with a damp cloth. And the other set was removed from the oven. The dried samples were then cooled in a desiccator for 30–40 min. Then both sets of samples were tested for compressive strength (Figure 2).

Figure 2 demonstrates the most noticeable changes in compressive strength for the mixes M3, M4, and M7, especially for the mixes cured under Regime 2 (Figure 2b). However, 24-h exposure of M3 and M7 to an aqueous medium resulted in a drop in compressive strength, and for M4 the same exposure conditions enabled an increase in strength. For M3 and M7 cured under Regime 1, the drop in compressive strength was 57% and 31%, respectively (Figure 2a), whereas the same mixes cured under Regime 2 showed reductions in compressive strength of 38% and 16%, respectively (Figure 2b). Thus, hydrothermal curing conditions (Regime 2) promote improved water resistance of these mixes. In turn, for Mix 4, 24-h exposure to an aqueous medium promoted strengthening of the structure under application of both Regime 1 and Regime 2. This was confirmed by the increase in compressive strength for M4 by 74% and 43% when cured under Regime 1 and 2, respectively. Additionally, for M5 and M6, despite their low compressive strength (not higher than 0.7 MPa), the 24-h exposure to an aqueous medium negatively affected the compressive strength results. For M5, cured under Regime 1, 24-h exposure to an aqueous environment resulted in complete destruction of the samples. For M5 when cured under Regime 2, there was a 3.8% reduction in compressive strength. For M6, cured under Regime 1, the drop in compressive strength after 24-h exposure to an aqueous medium was 23%. However, the same mix, cured under Regime 2 showed zero strength, even without aging in a water environment. Thus, hydrothermal curing conditions (Regime 2) favorably affected the structure formation of mix M5 and negatively affected the structure formation of M6. In this paper, water resistance is expressed as the water resistance coefficient or fluxing coefficient K , which is the ratio of the compressive strength of samples saturated with water (R_2) to the compressive strength of the samples in a dry state (R_1). The fluxing coefficient/water resistance K is calculated by Equation (1):

$$K = \frac{R_2}{R_1} \quad (1)$$

where R_2 is the average compressive strength of water-saturated specimens, MPa; and R_1 is the average compressive strength of oven-dried specimens, MPa.

The analysis of water resistance data (Figure 3) shows that among the mixes cured under Regime 1, the mixes M1, M2 and M8 had zero water resistance (i.e., complete destruction in an aqueous medium). However, when the same mixes were subject to hydrothermal curing conditions (Regime 2), the water resistance values were increased significantly, except for mix M8. At the same time, curing under Regime 2 for M4 and M6 resulted in a decrease in water resistance and led to a complete failure in case of M6.

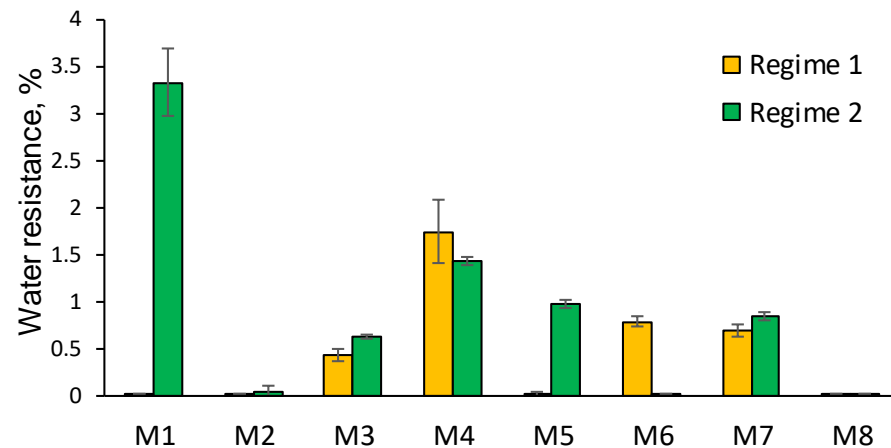


Figure 3. Water resistance of AAC cured in different regimes.

In terms of the effect of citrogypsum on water resistance performance of the AAC mixes, the following is observed:

- For the “GBFS-NaOH” system, the addition of citrogypsum (M7) cured under both Regimes: 1 and 2, resulted in a decrease in water resistance by 60% and 40%, respectively.
- For the “GBFS-Na₂CO₃” system, the addition of citrogypsum (M6) promoted an increase in water resistance up to 83%, when cured under Regime 1. However, when cured under Regime 2, the addition of citrogypsum caused a drastic drop in water resistance up to a complete failure of the samples.
- For the “GBFS-Na₂SiO₃” system, the incorporation of citrogypsum (M8) resulted in a reduction in water resistance from 0.96 to zero when cured under Regime 2.

3. Materials and Methods

3.1. Materials

GBFS derived from a Russian metallurgic plant was used as the main aluminosilicate component in the study. Citrogypsum was used in the work as a gypsum-bearing supplementary mineral additive. Citrogypsum is a waste product of the biochemical production of citric acid, and formed as a result of the microbiological synthesis of chalk mass using a culture of *Aspergillus niger*, i.e., industrial gypsum waste (GW). Citrogypsum consists mainly of a hydrated form of calcium sulphate CaSO₄·2H₂O with the traces of citric acid not exceeding 1%. The choice of citrogypsum as a recycled mineral additive in AAC is justified by the following reasons:

- The absence of P₂O₅ and F components in citrogypsum, which are typically present in PG. These components negatively affect hardening processes in binding systems;
- The need to alienate large areas to build new landfills. Underutilized reserves of citrogypsum in Russia today account for 351 K m³, which occupy an area of about 58.5 Km²;
- The undesirability of storing citrogypsum in open landfills due to elevated volumes of such toxic metals as Al, P, SO₃, Zr, Ce, etc., which can easily leach into soils and groundwater or be emitted to the atmosphere (in the case of volatile compounds), causing serious environmental problems;

- The incorporation of citrogypsum in the GBFS-based AACs as a supplementary source of alkaline elements, mainly Ca^{2+} cations, which enable chemical activation and further hydration reaction of GBFS.

The natural appearance and SEM-images of GBFS and citrogypsum in their original state are shown in Figure 4.



Figure 4. Natural appearance (a) and SEM-images (b) of GBFS and citrogypsum.

Several alkaline activators used in the study are listed below:

- Sodium alkali metal salts in form of sodium carbonate Na_2CO_3 and sodium liquid glass Na_2SiO_3 ;
- Sodium alkali metal hydroxide in form of caustic soda NaOH (98% purity).

3.2. Methods

The chemical compositions of the studied industrial by-products citrogypsum and GBFS were determined by X-ray fluorescence analysis (XRF) using an X-ray workstation WorkStation ARL 9900 (Thermo Scientific, Waltham, MA, USA), with Co-anode radiation.

Based on the determined chemical composition (Table 3), GBFS is characterized by a rather high content of oxides of alkaline earth metals ($\text{CaO} + \text{MgO} > 48\%$). At the same time, the presence of alkali metal oxides $\text{Na}_2\text{O} + \text{K}_2\text{O}$ does not exceed 1%. The content of SiO_2 and Al_2O_3 oxides reaches 39.7% and 9.48%, respectively. Thus, the ratio of basic oxides in GBFS makes it possible to draw an analogy with the chemical composition of OPC. Therefore, for the studied GBFS, the manifestation of hydraulic activity is likely, and there is a possibility for its use as an independent binding component.

Table 3. Chemical composition of GBFS and citrogypsum.

Component	Oxides Content, (wt.%)													
	CaO	SiO ₂	Al ₂ O ₃	MgO	Na ₂ O	K ₂ O	TiO ₂	Fe ₂ O ₃ /FeO	MnO	SrO	Cl	P ₂ O ₅	ZrO ₂	CeO ₂
GBFS	40.7	39.7	9.48	7.58	0.56	0.54	0.35	0.22	0.55	0.14	0.05	–	0.01	0.02
Citrogypsum	43.3	0.54	0.13	0.06	55.5	0.04	0.03	–	0.15	–	0.14	–	0.08	–

Chemical composition of the citrogypsum, to a greater extent, is represented by CaO and SO₃ oxides, which in total make up ≈99%. In other words, citrogypsum fully corresponds to NG and consists of hydrated form of calcium sulfate CaSO₄ with traces of Fe₂O₃/FeO, SiO₂, and Al₂O₃, which together do not exceed 1%. With this chemical composition, citrogypsum compares favorably with its closest analogue phosphogypsum (PG), which is a waste product of sulfuric acid production of mineral fertilizers (double superphosphate, ammonium phosphate precipitate, etc.), formed in the process of sulfuric acid processing of natural apatites and phosphorites into phosphoric acid. Due to the peculiarities of the production technology, PG contains P₂O₅ and F, which contribute to lower reactivity in the binder system during hardening [28].

Sieve analysis. For a more accurate and quantitative assessment of the granulometry, citrogypsum and GBFS were subject to sieve analysis according to the method presented in the Russian Standard GOST 8735-88 “Sand for construction work. Test Methods”.

Partial residues (a_i) were determined by Equation (2):

$$a_i = \frac{100 \cdot m_1}{m_0} \quad (2)$$

where m_0 is the sample weight, g; and m_1 is the weight of the residue on the i -th sieve, g.

The total residue on each sieve (A_i) in percent was determined by Equation (3):

$$A_i = a_{2.5} + a_{1.25} + \dots + a_i \quad (3)$$

where $a_{2.5}, a_{1.25}, \dots, a_i$ are partial residues on the corresponding sieves.

Fineness modulus (M_k) without grains larger than 5 mm was calculated according to Equation (4):

$$M_K = \frac{A_{2.5} + A_{1.25} + A_{0.63} + A_{0.315} + A_{0.16}}{100} \quad (4)$$

where $A_{2.5}, A_{1.25}, A_{0.63}, A_{0.315}, A_{0.16}$ are total residues on the sieves with mesh diameters of 2.5, 1.25, 0.63, 0.315, and 0.16 mm, respectively, %.

Based the analysis, the grain size composition and fineness modulus M_k of the GBFS and citrogypsum were obtained and are presented in Table 4 and Figure 6.

A comparison of the sieve analysis results for GBFS and citrogypsum showed that more than 95% of GBFS particles were in the size range of 0.315–1.25 mm. At the same time, ≈40% of the citrogypsum particles fell into the range of less than 0.16 mm. The remaining 60% were evenly distributed in the range of 0.1–5 mm, i.e., they had a much wider spread in size vs. GBFS particles. However, particle size of GBFS, in general, was significantly shifted to the zone of larger particles vs. citrogypsum, with characteristic values of M_k of 3.46 and 2.15 for GBFS and citrogypsum, respectively.

Table 4. Granulometry and fineness modulus of the GBFS and citrogypsum.

Residue Type		Sieve Residue, wt.%,							Fineness Modulus (Mk)
GBFS									
Mesh, mm	5	2.5	1.25	0.63	0.315	0.16	0.08	<0.08	3.46
Partial residue, wt.%	0.3	1.7	68.6	10.5	14.1	3	0.9	0.1	
Total residue, wt.%	0.3	2	70.6	81.1	95.2	98.2	99.1	99.2	
Citrogypsum									2.15
Mesh, mm	5	2.5	1.25	0.63	0.315	0.16	0.08	<0.08	
Partial residue, wt.%	16.5	8.9	7.4	10.5	9.2	8.9	38.56	0	
Total residue, wt.%	16.5	25.4	32.8	43.3	52.5	61.4	100	100	

In this regard, to further study GBFS, it was ground in a ball mill RMSH-200, 50 l (Figure 5). The grinding process was carried out in a dry environment for 2.5 h.

**Figure 5.** Ball mill and grinding bodies used to grind GBFS.

Uralite cylinders 35 × 35 mm in size were used as grinding bodies. They exclude undesirable yield from milling into the crushed material. The ratio of grinding media to ground material was 5:1.

Granulometry. Granulometric analysis of GBFS ground in a ball mill and citrogypsum was carried out by laser granulometry using an ANALYSETTE 22 NanoTec plus laser particle analyzer (Fritsch, Markt Einersheim, Germany), which estimated the particle size in the range from 0.2 to 600 µm for 40 fractions (Figure 6).

The granulometric analysis showed that particles of the ground GBFS product are generally distributed within the range from 5 to 80 µm, and for citrogypsum, two peaks were revealed in the ranges from 20 to 200 µm and from 500 to 700 µm.

According to the results obtained with the Blaine machine PSH-12, ground GBFS and citrogypsum products had a specific surface area of 4.5 cm²/g and 2.9 cm²/g, respectively. The specific gravity (SG) of ground GBFS and citrogypsum was 3 and 2.4, respectively.

The milling of GBFS product made it possible to ensure similar granular characteristics of both GBFS and citrogypsum product.

The SG is the ratio of a material's density ($\rho_{material}$) with that of water (ρ_{water}) at 4 °C (where it is most dense and is taken to have the value 999.974 kg/m³). It is, therefore, a relative quantity with no units.

The SG of the raw materials was calculated with Equation (5):

$$SG = \frac{\rho_{material}}{\rho_{water}} \quad (5)$$

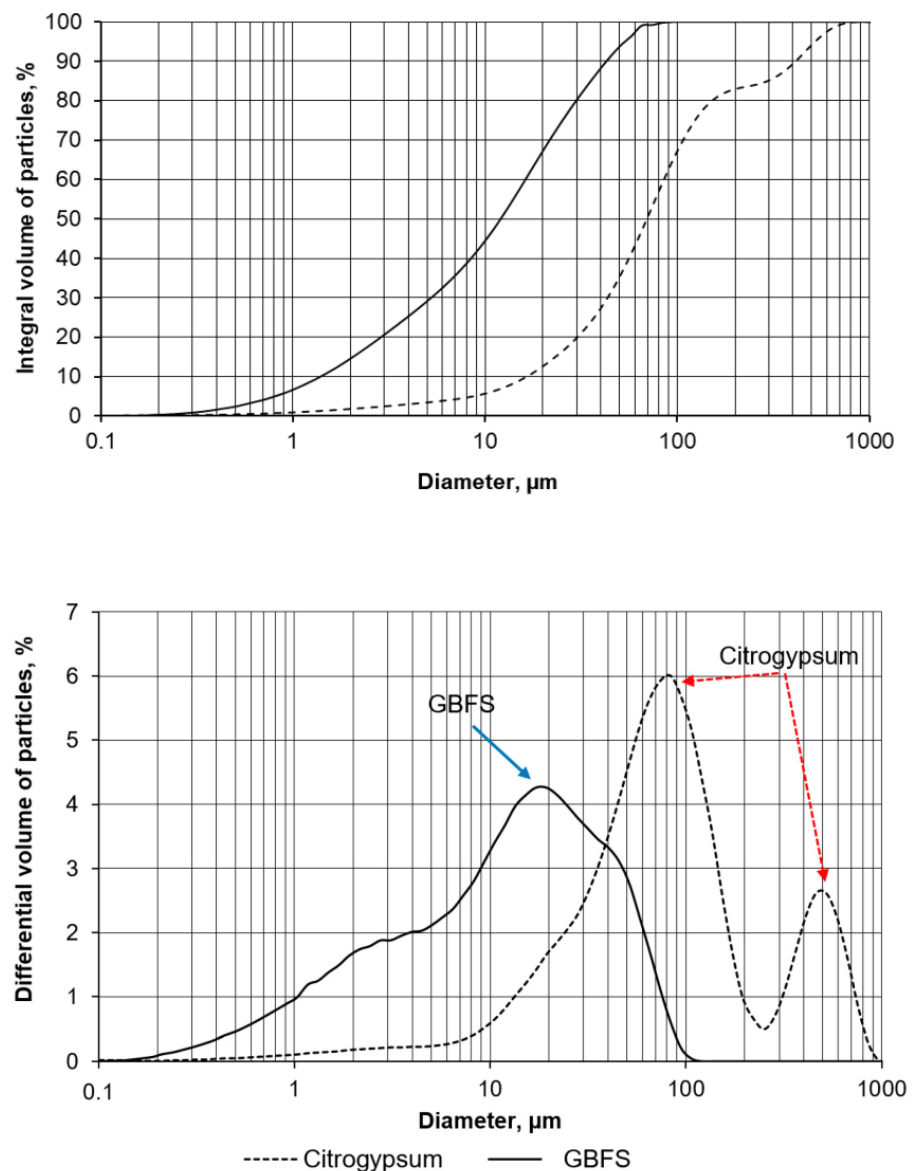


Figure 6. Granulometry of citrogypsum and ground GBFS.

3.3. Sample Preparation

Two sets of AAC cube specimens with different mix compositions were prepared. Each mix had three replicates. Experimental mixes differed by type of activating agent, as well as by the presence/absence of citrogypsum. The systems “GBFS-water” and “GBFS-citrogypsum-water” were considered as reference mixes. The compositions of the experimental AAC mixes are shown in Table 2. In the compositions with citrogypsum (M2, M6–8), GBFS was replaced with 5% of citrogypsum. Alkaline activators were used at the rate of 5% of total weight of solid content (GBFS + citrogypsum + alkaline activator) of AAC.

Two sets of experimental mixes were prepared then cured under different regimes, as depicted in Figure 7.

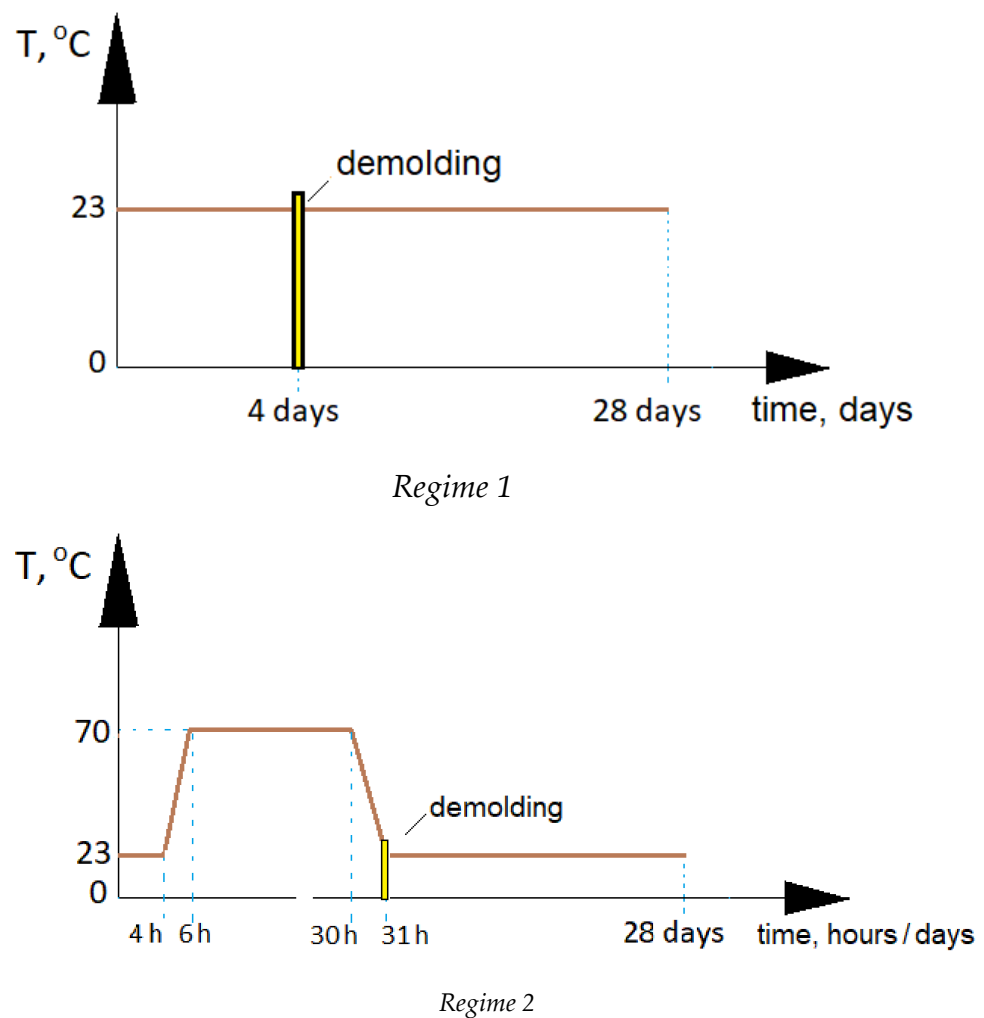


Figure 7. Scheme of the curing regimes.

Regime 1: Curing in ambient conditions with relative humidity (RH) $\approx 42\%$ and temperature $23 \pm 3^{\circ}\text{C}$ for 4 days \rightarrow demolding and further curing in ambient conditions until testing at the ages of 4, 7, and 28 days were performed.

Regime 2: Curing in ambient conditions with RH $\approx 42\%$ and temperature $23 \pm 3^{\circ}\text{C}$ for 4 h, followed by placement in a steaming chamber \rightarrow gradual temperature rise in the chamber to 70°C for 1–1.5 h \rightarrow isothermal conditioning at 70°C for 24 h \rightarrow cooling in the chamber to ambient temperature for 1 h \rightarrow demolding \rightarrow further curing in ambient conditions with RH $\approx 42\%$ and temperature $23 \pm 3^{\circ}\text{C}$ until testing at the ages of 4, 7 and 28 days was performed.

The samples cured under Regime 1 reached the demolding strength on the 4th day, whereas the samples cured in Regime 2 reached demolding strength after 31 h. After demolding, the samples were further tested at 4, 7 and 28 days of curing.

4. Conclusions

It was found that hydrothermal curing (Regime 2) provides more favorable conditions than ambient curing (Regime 1) for the formation of a strong cementitious structure in GBFS-based AACs activated with Na_2CO_3 , NaOH and Na_2SiO_3 . A similar effect was also observed for the reference mix M2, which contained citrogypsum and did not have alkaline activation.

For the mixes activated with Na_2SiO_3 , hydrothermal curing (Regime 2) and the addition of citrogypsum to AAC did not show any significant effect on compressive strength.

In this case, all the experimental mixes which were subject to either of the curing regimes the compressive strength values did not exceed 2 MPa.

The addition of citrogypsum led to a negative effect on the strength properties of all the experimental AAC mixes after either of the curing regimes was applied, except for the mix activated with NaOH (M7).

The mixes with citrogypsum were characterized by a looser framework structure, and demonstrated a significant drop in strength and SG in comparison with mixes free of citrogypsum.

The mixes M4 and M7 activated with NaOH demonstrate the highest strength, SG and water resistance, regardless of the curing conditions and curing time.

A study on the effect of citrogypsum through 28 days for the AAC mixes showed that the incorporation of citrogypsum resulted in a drop in SG from 4% to 30%, and the reduction in compressive strength was from 1.3 MPa to a complete failure.

The addition of citrogypsum affected the water-resistant properties of the AACs differently:

- NaOH-activated AAC systems with citrogypsum cured under both Regime 1 and Regime 2 resulted in a decrease in water resistance by 60% and 40%, respectively;
- Citrogypsum in Na_2CO_3 -activated AAC systems promoted an improvement in water resistance by up to 83% when cured under Regime 1. However, with Regime 2, the addition of citrogypsum caused a drastic drop in water resistance up to complete failure;
- The addition of citrogypsum in Na_2SiO_3 -activated AAC systems resulted in a reduction in water resistance from 0.96 to zero when Regime 2 was applied.

When citrogypsum was added, the highest water resistance (0.77) was observed for the mix M6 activated with Na_2CO_3 cured in ambient conditions (Regime 1). When cured under Regime 2, M7 activated with NaOH had the highest water resistance (0.84). However, for M6 activated with Na_2CO_3 and cured under Regime 1, the presence of citrogypsum had a positive effect on water resistance. In this case, water resistance showed an 83% improvement for the mix M6 activated with Na_2CO_3 in comparison with the mix M3 which did not contain citrogypsum.

Overall, the alkaline activator and curing regime are both crucial factors that govern the response of citrogypsum as a supplementary mineral additive in GBFS-based AAC compositions in regards to compressive strength, specific gravity and water resistance.

Author Contributions: Conceptualization, N.I.K. and M.I.K.; methodology, N.I.K., I.S.N. and N.I.A.; validation, N.I.K., M.I.K. and A.I.K.; formal analysis, I.S.N. and N.I.A.; investigation, N.I.A., I.S.N., N.I.K. and M.I.K.; resources, A.I.K., N.I.K., R.A.G. and I.S.N.; data curation, M.I.K.; writing—original draft preparation, N.I.K., M.I.K. and N.I.A.; writing—review and editing, N.I.K., N.I.A. and M.I.K.; visualization, I.S.N., A.I.K., R.A.G. and N.I.K.; supervision, N.I.K. and M.I.K.; project administration, N.I.A. and N.I.K.; funding acquisition, N.I.K. and I.S.N. All authors have read and agreed to the published version of the manuscript.

Funding: The work was realized under support of the State Assignment for the creation of new laboratories in 2021, including under the guidance of young promising researchers of the national project “Science and Universities”. The research project title is “Development of scientific and technological foundations for the creation of an integrated technology for processing gypsum-containing waste from various industrial enterprises”, FZWG-2021-0017.

Data Availability Statement: Not applicable.

Acknowledgments: The work was realized with the administrative support of the world-class scientific and educational center “Innovative Solutions in the Agricultural Sector” (Belgorod), using equipment of the High Technology Center at BSTU named after V. G. Shukhov.

Conflicts of Interest: The authors declare no conflict of interest.

References

- Berardi, U. A cross-country comparison of the building energy consumptions and their trends. *Resour. Conserv. Recycl.* **2017**, *123*, 230–241. [CrossRef]
- Sousa, V.; Bogas, J.A. Comparison of energy consumption and carbon emissions from clinker and recycled cement production. *J. Clean. Prod.* **2021**, *306*, 127277. [CrossRef]
- One Planet Network Webpage. Analysis of the Construction Value Chain. 2021. Available online: https://www.oneplanetnetwork.org/sites/default/files/value-chain_analysis_-_construction_-_210210.pdf (accessed on 2 February 2023).
- Pirieva, S.Y.; Alfimova, N.I.; Voropaev, V.S.; Kozhukhova, N.I. Biosafety Gypsum Binder Based on Gypsum-Bearing Waste. *IOP Earth Environ. Sci.* **2022**, in press.
- Kozhukhova, N.I.; Lebedev, M.S.; Vasilenko, M.I.; Goncharova, E.N. Ecology-toxicology study of low-calcium solid wastes from power plants. *Int. J. Pharm. Technol.* **2016**, *8*, 15349–15360.
- Kozhukhova, N.I.; Lebedev, M.S.; Vasilenko, M.I.; Goncharova, E.N. Fly Ash Impact from Thermal Power Stations on the Environment. *J. Phys. Conf. Ser.* **2018**, *1066*, 012010. [CrossRef]
- Kozhukhova, N.I.; Lebedev, M.S.; Vasilenko, M.I.; Goncharova, E.N. Toxic Effect of Fly Ash on Biological Environment. *IOP Conf. Ser. Earth Environ. Sci.* **2019**, *272*, 022065. [CrossRef]
- Vasilenko, M.I.; Lebedev, M.S.; Goncharova, E.N.; Kozhukhova, N.I.; Kozhukhova, M.I. The study of ecological impact of fly ash-based geopolymer binders on soil and aquatic biota. *IOP Conf. Ser. Mater. Sci. Eng.* **2020**, *791*, 012049. [CrossRef]
- Tolypin, D.A.; Tolypina, N.M. The effect of polydisperse concrete scrap of 3D printing on the structure formation of concrete. *Bull. BSTU Named V.G. Shukhov.* **2021**, *7*, 17–23. [CrossRef]
- Bakhtin, A.S.; Lyubomirsky, N.V.; Fedorkin, S.I.; Bakhtina, T.A.; Belenko, G.R. The influence of forced carbonization on the properties of gypsum-lime systems based on secondary raw materials. *Constr. Mater. Prod.* **2021**, *4*, 69–81. [CrossRef]
- Ajith, A.; Raveendran, K.G. Effect of Chemically Activated Fly Ash on Concrete. Proceedings of SECON'19. *Struct. Eng. Constr. Manag.* **2019**, *46*, 221–235. [CrossRef]
- Wang, S.; Llamazos, E.; Baxter, L.; Fonseca, F. Durability of biomass fly ash concrete: Freezing and thawing and rapid chloride permeability tests. *Fuel* **2008**, *87*, 359–364. [CrossRef]
- Al-Luhybi, A.S.; Qader, D.N. Mechanical Properties of Concrete with Recycled Plastic Waste. *Civ. Environ. Eng.* **2021**, *17*, 629–643. [CrossRef]
- Kishan, L.J.; Sancheti, G.; Kumar Gupta, L. Durability performance of waste granite and glass powder added concrete. *Constr. Build. Mater.* **2020**, *252*, 119075. [CrossRef]
- Godinho-Castro, A.P.; Testolin, R.; CJanke, L.; Corr  a, A.X.R.; Radetski, C.M. Incorporation of gypsum waste in ceramic block production: Proposal for a minimal battery of tests to evaluate technical and environmental viability of this recycling process. *Waste Manag.* **2012**, *32*, 153–157. [CrossRef]
- Chernysh, Y.; Yakhnenko, O.; Chubur, V.; Roub  k, H. Phosphogypsum Recycling: A Review of Environmental Issues, Current Trends, and Prospects. *Appl. Sci.* **2021**, *11*, 1575. [CrossRef]
- Su  rez, S.; Roca, X.; Gasso, S. Product-specific life cycle assessment of recycled gypsum as a replacement for natural gypsum in ordinary Portland cement: Application to the Spanish context. *J. Clean. Prod.* **2016**, *117*, 150–159. [CrossRef]
- Silgado, S.S.; Valdiviezo, L.J.C.; Domingo, S.G.; Roca, X. Multi-criteria decision analysis to assess the environmental and economic performance of using recycled gypsum cement and recycled aggregate to produce concrete: The case of Catalonia (Spain). *Resour. Conserv. Recycl.* **2018**, *133*, 120–131. [CrossRef]
- Pedre  o-Rojas, M.A.; Fo  rt, J.;   ern  y, R.; Rubio-de-Hita, P. Life cycle assessment of natural and recycled gypsum production in the Spanish context. *J. Clean. Prod.* **2020**, *253*, 120056. [CrossRef]
- Bumanis, G.; Korjakins, A.; Bajare, D. Environmental Benefit of Alternative Binders in Construction Industry: Life Cycle Assessment. *Environments* **2022**, *9*, 6. [CrossRef]
- Degirmenci, N.; Okucu, A.; Turabi, A. Application of phosphogypsum in soil stabilization. *Build. Environ.* **2007**, *42*, 3393–3398. [CrossRef]
- Wirsching, F.; H  ller, R.; Olejnik, R. FGD definitions and legislation in the European Communities, in the OECD and in Germany. *Stud. Environ. Sci.* **1994**, *60*, 205–216. [CrossRef]
- Leiva, C.; Arenas, C.G.; Vilches, L.F.; Vale, J.; Gimenez, A.; Ballesteros, J.C.; Fern  ndez-Pereira, C. Use of FGD in fire resistant panels. *Waste Manag.* **2010**, *30*, 1123–1129. [CrossRef]
- Zhang, Y.C.; Dai, S.B.; Huang, J.; Duan, S.G.; Zhi, Z.Z. Preparation of thermal insulation plaster with FGD. *Kemija u Industriji   asopis Kemi  ara i Kem. In  enjera Hrvat.* **2016**, *65*, 283–288. [CrossRef]
- Voropaev, V.; Alfimova, N.; Nikulin, I.; Nikulicheva, T.; Titenko, A.; Nikulichev, V. Influence of Gypsum-Containing Waste on Ammonia Binding in Animal Waste Composting. *Agriculture* **2021**, *11*, 1153. Available online: <https://www.mdpi.com/journal/agriculture> (accessed on 2 February 2023). [CrossRef]
- Kosti  -Pulek, A.; Slobodanka, R.M.; Logar, V.; Tomanec, R.; Popov, S. Production of calcium sulphate alpha-hemihydrate from citrogypsum in unheated sulphuric acid solution. *Ceramics-Silicaty* **2000**, *44*, 104–108. Available online: https://www.researchgate.net/publication/235559480_Production_of_calcium_sulphate_alpha-hemihydrate_from_citrogypsum_in_unheated_sulphuric_acid_solution (accessed on 2 February 2023).

27. Ozkul, M.H. Utilization of citro- and desulphogypsum as set retarders in Portland cement. *Cem. Concr. Res.* **2000**, *30*, 1755–1758. [[CrossRef](#)]
28. Kozhukhova, N.I.; Shurakov, I.M.; Kozhukhova, M.I.; Elistratkin, M.Y.; Alfimova, N.I. Understanding the relationship between composition and rheology in alkali-activated binders. *J. Phys. Conf. Ser.* **2021**, *2124*, 012004. [[CrossRef](#)]
29. Duxson, P. 3—*Geopolymer Precursor Design*. *Geopolymers*; Woodhead Publishing: Amsterdam, The Netherlands, 2009; pp. 37–49. [[CrossRef](#)]
30. Xie, Z.; Xi, Y. Hardening mechanisms of an alkaline-activated class F fly ash. *Cem. Concr. Res.* **2001**, *31*, 1245–1249. [[CrossRef](#)]
31. Douglas, E.; Bilodeau, A.; Malhotra, V. Properties and durability of alkali activated slag concrete. *ACI Mater. J.* **1992**, *89*, 509–516.
32. Granizo, M.L.; Blanco-Varela, M.T.; Palomo, A. Influence of the starting kaolin on alkali-activated materials based on metakaolin. Study of the reaction parameters by isothermal conduction calorimetry. *J. Mater. Sci.* **2000**, *35*, 6309–6315. [[CrossRef](#)]
33. Shi, C.; Day, R.L. Some factors affecting early hydration of alkali-slag cements. *Cem. Concr. Res.* **1996**, *26*, 439–447. [[CrossRef](#)]
34. Collins, F.; Sanjayan, J.G. Early age strength and workability of slag pastes activated by NaOH and Na₂CO₃. *Cem. Concr. Res.* **1998**, *28*, 655–664. [[CrossRef](#)]
35. Alfimova, N.I.; Pirieva, S.Y.; Elistratkin, M.Y.; Nikulin, I.S.; Titenko, A.A. Using of gypsum-bearing by-products in construction material fields. *Bull. BSTU Named V.G. Shukhov.* **2020**, *8*, 8–25. [[CrossRef](#)]
36. Guo, X.; Shi, H.; Chen, L.; Dick, W.A. Alkali-activated complex binders from class C fly ash and Ca-containing admixtures. *J. Hazard. Mater.* **2010**, *173*, 480–486. [[CrossRef](#)]
37. Maierdan, Y.; Aminul Haque, M.; Chen, B.; Maimaitiyiming, M.; Riaz Ahmad, M. Recycling of waste river sludge into unfired green bricks stabilized by a combination of phosphogypsum, slag, and cement. *Constr. Build. Mater.* **2020**, *260*, 120666. [[CrossRef](#)]
38. Liu, Z.; Chen, Q.; Xie, X.; Xue, G.; Du, F.; Ning, Q.; Huang, L. Utilization of the sludge derived from dyestuff-making wastewater coagulation for unfired bricks. *Constr. Build. Mater.* **2011**, *25*, 1699–1706. [[CrossRef](#)]
39. Rashad, A.M. Potential use of phosphogypsum in alkali-activated fly ash under the effects of elevated temperatures and thermal shock cycles. *J. Clean. Prod.* **2015**, *87*, 717–725. [[CrossRef](#)]
40. Vaičiukynienė, D.; Nizevičienė, D.; Kiele, A.; Janavičius, E.; Pupeikis, D. Effect of phosphogypsum on the stability upon firing treatment of alkali-activated slag. *Constr. Build. Mater.* **2018**, *184*, 485–491. [[CrossRef](#)]

Disclaimer/Publisher's Note: The statements, opinions and data contained in all publications are solely those of the individual author(s) and contributor(s) and not of MDPI and/or the editor(s). MDPI and/or the editor(s) disclaim responsibility for any injury to people or property resulting from any ideas, methods, instructions or products referred to in the content.